# Ground-State Properties of the Two-Dimensional Bose Coulomb Liquid

W. R. Magro and D. M. Ceperley

*National Center for Supercomputing Applications, Department of Physics, University of Illinois, Urbana, Illinois 61801*

(Received 19 April 1994)

We present results of a ground-state study, via the diffusion Monte Carlo method, of a two-dimensional charged boson liquid. We observe three distinct behaviors in this system. At the lowest densities a close-packed Wigner crystal forms. At $r_s \approx 12$ the crystal melts into a noncondensed liquid exhibiting algebraic off-diagonal long-range order; the single-particle density matrix decays as $r^{-r_s/4}$. Above a threshold density ($r_s < 8$), the long-wavelength momentum distribution diverges as $k^{(r_s-8)/4}$, although no condensate forms.

PACS numbers: 61.20.Ja, 67.40.Db

Thermal fluctuations are known to destroy long-range order in one- and two-dimensional homogeneous systems [1–3]. Pitaevskii and Stringari [4], by deriving a generalized uncertainty relation for non-Hermitian operators, have elegantly demonstrated the absence of a condensate *even at zero temperature* in interacting homogeneous 1D Bose systems. When the $f$-sum rule [5] holds, an important consequence of this relation is the inequality,

$$n_k \geq \frac{n_0}{4S_k} - \frac{1}{2}, \tag{1}$$

involving the momentum distribution $n_k$, structure factor $S_k$, and condensate fraction $n_0$. Using this inequality we show that, for a system of bosons interacting through a two-dimensional Coulomb pair potential, the predominance of long-wavelength plasmons rules out the existence of a condensate in the thermodynamic limit. Campbell, considering the role of the plasmons, apparently first suggested this model might possess no Bose condensate [6]. Next, employing the diffusion Monte Carlo method, we confirm the long-wavelength plasmon structure, explicitly calculate the single-particle density matrix, and locate the transition density for Wigner crystallization.

The ground state of the 2D Bose Coulomb liquid (2DBCL) is closely related to the bosonic representation of the Laughlin wave function, used to study the fractional quantum Hall effect [7]. In an approach analogous to that introduced by Gaskell [8], Kane *et al.* [9] have shown that Laughlin's wave function contains long wavelength correlations appropriate to the quantum 2DBCL. Girvin and MacDonald have shown that this wave function exhibits algebraic long-range order [10], so the 2DBCL ground state should also exhibit this behavior [9]. Although the long distance physics of these systems is identical, the short-range behavior is quite distinct. A key feature of Laughlin's wave function is that the probability for two particles to overlap vanishes, as is appropriate for *classical* 2D charges. In the 2DBCL, however, quantum mechanics blurs the Coulomb core, yielding a depressed but finite probability for such a configuration.

When electrons are immersed in a magnetic field, cyclotron oscillations suppress long-range charge density fluctuations. Pitaevskii and Stringari have applied Eq. (1) to show that this suppression leads to increased fluctuations in the boson field operators which in turn destroy the Bose condensate [11]. In the sequel we show that the plasmons are the relevant excitations in the zero field 2DBCL, suppressing long-wavelength density fluctuations and destroying the condensate.

We consider the ground state of a periodic system of $N$ bosons each of charge $+q$ in two dimensions and embedded in a neutralizing background. The pairs interact with a repulsive 2D Coulomb potential, $-q^2 \ln r$. We emphasize that, unlike in a 2D electron system, this is a true Coulomb interaction. That is $V_k = 2\pi/k^2$, the solution to the 2D Poisson equation, $\nabla^2 V(\mathbf{r}) = -2\pi\delta(\mathbf{r})$. We work in reduced units: lengths are given in units of $r_s a$, and energies in units of $q^2$, so the Hamiltonian is

$$\mathcal{H} = -\sum_i \frac{1}{r_s^2}\nabla_i^2 - \sum_{i<j} \ln(r_{ij}), \tag{2}$$

where $i,j$ are particle indices, $a$ is a fixed reference length, and the free parameter $r_s$ is defined by $\pi(r_s a)^2 \equiv \Omega/N$, the inverse physical density. The unitless density is therefore always $\pi^{-1}$. The 2D Coulomb liquid admits plasma oscillations of frequency $\omega_p = 2/r_s$.

At sufficiently high density, the kinetic energy dominates the soft-core potential, yielding a liquid ground state, $\phi$, with condensate fraction $0 \leq n_0 \leq 1$. As our potential is velocity independent, the $f$-sum rule and relation (1) hold. In an isotropic system, the momentum distribution $n_k$ satisfies the normalization condition

$$\frac{1}{\Omega}\sum_{\mathbf{k}\neq 0} n_k = \int_{0+}^{\infty} \frac{k\,dk}{2\pi} n_k = 1 - n_0. \tag{3}$$

Assuming plasmons are the dominant long-wavelength excitations, the dynamic structure factor is $S(k \to 0, \omega) = A(k)\delta(\omega - \omega_p)$. From the $f$-sum rule and $S_k \equiv \int_0^\infty d\omega\, S(k,\omega)$ we find

$$S_{k\to 0} = \frac{k^2}{2r_s} = \frac{k^2}{r_s^2 \omega_p}. \tag{4}$$



0031-9007/94/73(6)/826(4)$06.00

From Eqs. (1), (3), and (4), the assumption of a condensate then leads to a $k^{-2}$ divergence in $n_k$ at long wavelengths and the immediate conclusion $n_0 = 0$.

We can understand the disappearance of the condensate by considering the Fourier transform of the momentum distribution, the single-particle density matrix,

$$n(\mathbf{r}) = \int dR \psi(R : \mathbf{r}_i + \mathbf{r}) \psi(R) \quad (5)$$

$$= \left\langle \frac{\psi(R : \mathbf{r}_i + \mathbf{r})}{\psi(R)} \right\rangle_{\psi(R)^2}; \quad (6)$$

the notation $R : \mathbf{r}_i + \mathbf{r}$ specifies the configuration $R = \{\mathbf{r}_1, \ldots, \mathbf{r}_i, \ldots, \mathbf{r}_N\}$, with particle $i$ displaced from $\mathbf{r}_i$ to $\mathbf{r}_i + \mathbf{r}$. Brackets denote a statistical average over the probability distribution $\psi^2$. In an isotropic system, $n(\mathbf{r})$ depends only on the magnitude $r = |\mathbf{r}|$. The bosonic ground state wave function can be taken everywhere real and non-negative, so one easily verifies $n(r) \geq 0$, $n(0) = 1$, and $n_0 = n(r \to \infty)$ [12]. Existence of a condensate thus implies $n(r \to \infty) > 0$. We can think of $n(r)$ as the relative change in probability amplitude obtained when a single particle is displaced from $\mathbf{r}_i$ to $\mathbf{r}_i + \mathbf{r}$, averaged over likely system configurations. The repulsive pair interaction favors configurations where particles are uniformly spaced, with each surrounded by a correlation "hole." Choosing one such configuration, $R$, we consider the change in potential energy which results from a large single-particle displacement, $r \approx \sqrt{\Omega}$, where $\Omega$ is the area of the system. The near-uniform distribution of particles in the liquid implies the average potential felt by the displaced particle is only that of the correlation hole. The leading contribution is therefore the attractive potential due to a charge of equal magnitude and opposite sign located in the hole, so the energy change is of order $\ln\Omega$. In the thermodynamic limit, this energy diverges, so the wave function $\psi(R : \mathbf{r}_i + \mathbf{r})$ and $n(r \to \infty)$ must vanish, and no condensate forms.

We have performed variational (VMC) and exact diffusion Monte Carlo (DMC) simulations of this system in its ground state. VMC calculates an observable $\langle\psi|O|\psi\rangle$ by averaging $O(R)$ over the probability distribution, $\psi(R)^2$. The trial wave function $\psi$ is expressed as a function of a small number of parameters, which we vary to minimize the energy, $\langle\psi|\mathcal{H}|\psi\rangle$. DMC samples the mixed distribution, $\psi(R)\phi(R)$, where $\phi$ is the true ground state, by treating the Schrödinger equation as a diffusion equation with a source term, $V(R)$. The ground state energy is computed exactly in this scheme, while other properties are obtained using the "mixed" estimator, $\langle\psi|O|\phi\rangle$.

The details of our calculation are largely identical to those described in Ref. [13]. One important difference, however, is the addition of a long-ranged interaction. We treat the resulting periodic potential using Ewald sums, according to the prescription of Smith [14]. We do not consider dipole interactions with the external medium, so our simulations correspond to the limit of a charged liquid embedded in a 2D conductor.

The ground-state wave function of a system of interacting bosons is often well described by the Jastrow pair-product form [15,16], which we write in the form

$$-\ln\psi(R) = U(R) = \sum_{i<j} \alpha u_s(r_{ij}) + \sum_{\mathbf{k}} u_k \rho_{\mathbf{k}} \rho_{-\mathbf{k}}, \quad (7)$$

with $u_s$ a short-ranged correlation factor, $\alpha$ a variational parameter, $u_k$ a long-ranged factor, and the Fourier components of the density $\rho_{\mathbf{k}} = \sum_i e^{i\mathbf{k}\cdot\mathbf{r}_i}$. We use a short-ranged correlation of the form

$$u_s(r) = \frac{r_s^2}{4}\left[r^2 \ln r - \frac{r^2}{2} + 1\right] e^{-\gamma r^2}, \quad (8)$$

which satisfies the cusp condition imposed by the diverging interaction for vanishing pair separations. The choice of cutoff parameter $\gamma \approx 3$ gave good results.

For the long-range correlation, we invoke the random phase approximation (RPA), which neglects three-phonon terms, to determine an optimal trial function [8,17]. We do not make the RPA in our calculation, but only use it to guide our choice of trial wave function, which controls the efficiency of the DMC calculation. Minimizing the RPA energy with respect to $u_k$, we find

$$u_k = \frac{1}{2N}\left[-1 + \sqrt{1 + \frac{4r_s^2}{k^4} e^{-k^2/4}}\right], \quad (9)$$

$$u_{k\to 0} = -\frac{r_s}{2}\frac{2\pi}{\Omega k^2} = -\frac{r_s}{2} V_k, \quad (10)$$

which, at large separations, gives a correlation proportional to the potential, namely $-(r_s/2)\ln r$. An equivalent result may also be obtained through the paired-phonon analysis [18] and the single mode approximation [9]. The Gaussian cutoff in $u_k$ is introduced to limit its effects to long-range correlations, where the RPA is valid. This correlation explicitly puts long-wavelength plasmon structure in the trial wave function, yielding $S_{k\to 0} = k^2/2r_s$. Should the true ground-state structure differ, DMC calculations will reveal this discrepancy at small $k$. Figure 1 shows variational and DMC structure factors for the liquid at $r_s = 5$. The curve $k^2/2r_s$ is also plotted to indicate the plasmon structure expected from Eq. (4). The agreement at small $k$ is excellent. Further, if we perturb $u_k$, DMC restores the behavior $k^2/2r_s$, confirming the dominance of plasmon modes at small $k$.

To efficiently compute the single-particle density matrix $n(r)$ we use a method based on that of McMillan [19]. During the normal course of a Monte Carlo simulation, we sample configurations $R$ from the distribution $\psi^2(R)$. Periodically, we pick a point, $\mathbf{x}$, in the box at random. We treat this point as a hypothetical target position for each particle in turn, yielding contributions to

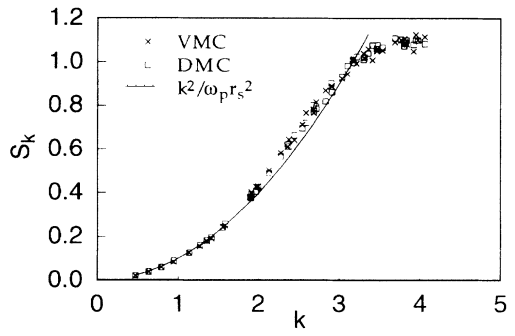


FIG. 1. Structure factors from the variational (VMC) and diffusion Monte Carlo (DMC) calculations at $r_s = 5$. The solid curve indicates the low momentum plasmon structure.

$n(r)$ at $N$ different displacements, $r = |\mathbf{x} - \mathbf{r}_i|$. Repeating this process throughout the simulation, we perform the required average over $\psi^2$ in VMC and $\psi\phi$ in DMC. The usual approach, according to Eqs. (5) and (7), involves an evaluation of the change in $U(R)$ resulting from a displacement of a particle and *all its periodic images*. Because the logarithmic potential is long ranged, we instead compute the change in $U(R)$ when a particle moves with its images fixed. In this case we replace $\Delta(R, \mathbf{r}_i, \mathbf{r}) \equiv U(R) - U(R : \mathbf{r}_i + \mathbf{r})$ with

$$\Delta'(R, \mathbf{r}_i, \mathbf{r}) \equiv \Delta(R, \mathbf{r}_i, \mathbf{r}) + \lim_{r \to 0} u_l(r) - u_l(r) + \sum_{\mathbf{k} \neq 0} u_k [e^{i\mathbf{k}\cdot\mathbf{r}} - 1], \quad (11)$$

where $u_l(r)$ is the Fourier transform of $u_k$. The correction $(\Delta' - \Delta)$ vanishes for $r = 0$ and in the thermodynamic limit, as it must.

From Eq. (9), the long-range correlation factor is proportional to the interaction and therefore logarithmic in $r$. At large separations, $u_l(r)$ dominates Eq. (11) with the result $\Delta'(R, \mathbf{r}_i, \mathbf{r} \to \infty) = (r_s/2) \ln r$. To analyze the long-range behavior of $n(\mathbf{r})$, we use the cumulant expansion [20],

$$\ln\langle e^x \rangle = \langle x \rangle + \tfrac{1}{2} \langle (x - \langle x \rangle)^2 \rangle + \cdots, \quad (12)$$

with $x$ a random variable. If $x$ is normally distributed, the expansion terminates at second order. We also note the identity

$$\langle e^{-2\Delta(R, \mathbf{r}_i, \mathbf{r})} \rangle = \left\langle \frac{\psi(R : \mathbf{r}_i + \mathbf{r})^2}{\psi(R)^2} \right\rangle_{\psi(R)^2} = 1. \quad (13)$$

Because $\Delta(R, \mathbf{r}_i, \mathbf{r})$ is the sum of $N - 1$ weakly correlated, bounded functions, the central limit theorem allows us to assume it is, to a good approximation, normally distributed. The functions are bounded because the Coulomb interaction has a soft core. With this assumption, Eqs. (12) and (13) yield

$$\langle [\Delta(R, \mathbf{r}_i, \mathbf{r}) - \langle \Delta(R, \mathbf{r}_i, \mathbf{r}) \rangle]^2 \rangle = -\langle \Delta(R, \mathbf{r}_i, \mathbf{r}) \rangle. \quad (14)$$

Equations (5), (12), and (14) then give

$$\ln[n(\mathbf{r})] = \tfrac{1}{2} \langle \Delta(R, \mathbf{r}_i, \mathbf{r}) \rangle. \quad (15)$$

We expect deviation from this behavior only near the crystallization density, where correlations become large. Finally, we obtain

$$n(r \to \infty) \propto \exp\{-\tfrac{1}{2} \langle \Delta'(R, \mathbf{r}_i, \mathbf{r}) \rangle\} = r^{-r_s/4}, \quad (16)$$

the expected algebraic long-range order.The results of our calculations are plotted in Fig. 2, where the asymptotic behavior of $n(r)$ follows Eq. (16). The upper curves in each pair show the results of the usual form, $n(r) = \langle e^{-\Delta(R, \mathbf{r}_i, \mathbf{r})} \rangle$, which curl up at the box edge due to the periodic nature of the wave function. For the lower curves, we have used Eq. (11) to eliminate these surface effects. Inspection of Eq. (16) reveals that $n_k$ diverges as $k^{(r_s - 8)/4}$, when $r_s < 8$. In the thermodynamic limit, the occupation of the zero momentum state diverges for these densities. It increases more slowly than the particle count, however, so the condensate fraction still vanishes.

In quantum solids there is also no condensate, so one might wonder at what density the charged particles prefer to localize rather than form a noncondensed liquid. Clearly, at very low density the liquid must freeze into a 2D Wigner crystal to minimize the dominant potential energy. We have computed the crystallization density by comparing energies for the liquid with those of a solid. We choose the triangular lattice, which has lower static energy than the square lattice. This choice also enables comparison with crystallization in the 2D Yukawa Bose liquid [13], a model for flux-lattice formation in high-temperature superconductors [21].

The trial wave function for a solid, $\psi_s$, is obtained from the liquid wave function by adding a Nosanow spring term [22], which effectively ties each particle to a lattice site, $\mathbf{Z}_i$:

$$\psi_s(R) = \psi_l(R) \prod_i e^{-c|\mathbf{r}_i - \mathbf{Z}_i|^2}, \quad (17)$$

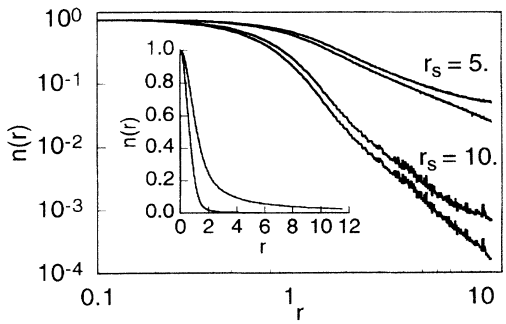


FIG. 2. The single-particle density matrix, $n(r)$, computed from diffusion Monte Carlo calculations of 154 particles. At each density, $r_s$, the upper curve results from the standard estimator, while our modified estimator gives the lower result [see Eq. (11)]. Inset: $n(r)$ plotted linearly.

with $c$ a variational parameter. Although not symmetric under particle exchange, this type of wave function gives excellent energies for many simple solids since exchange energies in quantum crystals are small. Because this wave function is typically better than the liquid wave function [13,23], a variational study would be ill suited to comparing liquid and solid energies. Use of DMC is hence important to eliminate this variational bias. For a system with long-range interactions in periodic boundary conditions, each particle forms a rectangular lattice with its own images, so one out of $N$ interactions is that appropriate to the static lattice rather than the bulk liquid. Finite-size effects in the crystal are substantially smaller and should also be a $1/N$ correction. Consequently, we assume a simple form for the finite-size scaling, $E_N = E_\infty + \chi/N$. The ground-state energies, $E_\infty$, listed in Table I, indicate crystallization occurs near $r_s = 12$. Should a different scaling law hold, our estimate of the crystallization density should not vary by more than $\approx \pm 1$. The short-range limit of a Yukawa potential is a Coulomb interaction, $K_0(r \to 0) = -\ln r$, so the crystallization density should equal that estimated by extrapolating calculations of the high-density Yukawa system [13], $r_s = 14.1$. Our method is not sensitive to the order of the phase transition, but an estimate of the transition width in the Yukawa liquid suggests it is weakly first order. Lindemann's ratio at melting is about $0.24 \pm 0.01$ in both systems.

In conclusion, we have found three different behaviors of the ground state of the 2D quantum Coulomb Bose liquid as a function of density. At small $r_s < 8$ the momentum distribution diverges as $k^{(r_s-8)/4}$. At larger $r_s$ it is bounded, but at $r_s \approx 12$ the system freezes. Although, in the thermodynamic limit, the ground state of this system is not condensed, superfluidity is nonetheless possible. We note that, because the plasmons are massive, this system has a finite critical superfluid velocity, in the sense of Landau and Lifshitz [24]. Path-integral calculations at finite temperature, or imaginary time diffusion constant studies in DMC, for example, could determine the superfluid density of this system. In the path-integral framework, where particles are mapped onto polymerlike rings, Bose condensation implies a nonvanishing probability for the two ends of a "cut" ring to wander arbitrarily far apart. Superfluidity, on the other hand, is simply expressed in terms of macroscopic particle exchange across the simulation cell. If the 2D Coulomb system is indeed superfluid, it may provide an ideal model system in which to study the differences between superfluidity and Bose condensation.

TABLE I. Extrapolated ground state energies calculated with DMC. Numbers in parentheses are estimated errors in the last decimal place. Calculations were performed for systems of 16 to 154 particles; $\alpha$ and $c$ are optimized variational parameters for a system of 16 particles.

| $r_s$ | $E_\infty/N$ | $\alpha$ | $c$ |
|---|---|---|---|
| | Liquid | | |
| 5.0 | −0.1540(4) | 0.87 | ... |
| 10.0 | −0.2500(2) | 1.09 | ... |
| 14.1 | −0.2818(4) | 1.15 | ... |
| | Crystal | | |
| 10.0 | −0.249 33(6) | 0.83 | 1.1 |
| 14.1 | −0.2840(3) | 0.85 | 1.5 |
| 20.0 | −0.3081(1) | 1.01 | 1.5 |

All of the calculations were performed on Cray, Sun, and HP computers at the National Center for Supercomputing Applications at the University of Illinois, Urbana. This work was supported by the National Science Foundation under Grant No. NSF-DMR 91-17822.

[1] R. E. Peierls, Ann. Inst. Henri Poincaré **5**, 177 (1935).
[2] P. C. Hohenberg, Phys. Rev. **158**, 383 (1967).
[3] N. D. Mermin, Phys. Rev. **176**, 250 (1968).
[4] L. Pitaevskii and S. Stringari, J. Low Temp. Phys. **85**, 377 (1991).
[5] D. Pines and P. Nozieres, *The Theory of Quantum Liquids, Volume I* (Addison-Wesley, Reading, MA, 1966).
[6] C. E. Campbell, in *Structure of Quantum Fluids*, edited by C. A. Croxton (J. Wiley and Sons, New York, 1978).
[7] R. B. Laughlin, Phys. Rev. Lett. **50**, 1395 (1983).
[8] T. Gaskell, Proc. Phys. Soc. **77**, 1182 (1961); **80**, 1091 (1962).
[9] C. L. Kane, S. Kivelson, D. H. Lee, and S. C. Zhang, Phys. Rev. B **43**, 3255 (1991).
[10] S. Girvin and A. MacDonald, Phys. Rev. Lett. **58**, 1252 (1987).
[11] L. Pitaevskii and S. Stringari, Phys. Rev. B **47**, 10915 (1993).
[12] O. Penrose and L. Onsager, Phys. Rev. **104**, 576 (1956).
[13] W. R. Magro and D. M. Ceperley, Phys. Rev. B **48**, 411 (1993).
[14] E. R. Smith, Molec. Phys. **45**, 915 (1982).
[15] A. Bijl, Physica (Utrecht) **7**, 869 (1940).
[16] Robert Jastrow, Phys. Rev. **98**, 1479 (1955).
[17] D. Ceperley, Phys. Rev. B **18**, 3126 (1978).
[18] Eugene Feenberg, *Theory of Quantum Fluids* (Academic Press, New York, 1969).
[19] W. L. McMillan, Phys. Rev. A **138**, 442 (1965).
[20] Milton Abromowitz and Irene A. Stegun, *Handbook of Mathematical Functions* (National Bureau of Standards, Gaithersburg, 1972).
[21] D. R. Nelson and S. Seung, Phys. Rev. B **39**, 9153 (1989).
[22] Lewis H. Nosanow and Gordon L. Shaw, Phys. Rev. **128**, 546 (1962).
[23] D. Ceperley, G. V. Chester, and M. H. Kalos, Phys. Rev. B **17**, 1070 (1978).
[24] L. D. Landau and E. M. Lifshitz, *Statistical Physics* (Addison-Wesley, Reading, MA, 1958).